Article

Neuron

Area-Specific Reestablishment of Damaged Circuits in the Adult Cerebral Cortex by Cortical Neurons Derived from Mouse Embryonic Stem Cells

Highlights

- ESC-derived cortical pyramidal neurons engraft in adult mouse lesioned cortex
- Grafted neurons display long-range patterns of connectivity with the host
- Transplant-derived patterns of projections are cortical area specific
- Integration requires a match in the areal identity of grafted and lesioned neurons

Authors

Kimmo A. Michelsen, Sandra Acosta-Verdugo, ..., Afsaneh Gaillard, Pierre Vanderhaeghen

Correspondence

afsaneh.gaillard@univ-poitiers.fr (A.G.), pierre.vanderhaeghen@ulb.ac.be (P.V.)

In Brief

Michelsen et al. show that transplanted cortical pyramidal neurons, derived from mouse pluripotent stem cells, can contribute to the reconstruction of an adult damaged cortical circuit. Successful integration requires a match in the areal identity of grafted and lesioned neurons.

Michelsen et al., 2015, Neuron *85*, 982–997
March 4, 2015
http://dx.doi.org/10.1016/j.neuron.2015.02.001

CellPress

CellPress

Neuron
Article

Area-Specific Reestablishment of Damaged Circuits in the Adult Cerebral Cortex by Cortical Neurons Derived from Mouse Embryonic Stem Cells

Kimmo A. Michelsen,[1,2,5] Sandra Acosta-Verdugo,[1,2,5,6] Marianne Benoit-Marand,[3] Ira Espuny-Camacho,[1,2] Nicolas Gaspard,[1,2] Bhaskar Saha,[3] Afsaneh Gaillard,[3,*] and Pierre Vanderhaeghen[1,2,4,*]
[1]Institut de Recherches en Biologie Humaine et Moléculaire (IRIBHM)
[2]ULB Neuroscience Institute (UNI)
Université Libre de Bruxelles (ULB), Campus Erasme, 808 Route de Lennik, 1070 Brussels, Belgium
[3]INSERM U1084, Experimental and Clinical Neurosciences Laboratory, Cellular Therapies in Brain Diseases Group, University of Poitiers, 1 rue Georges Bonnet, BP 633, 86022 Poitiers Cedex, France
[4]WELBIO, Université Libre de Bruxelles (ULB), Campus Erasme, 808 Route de Lennik, 1070 Brussels, Belgium
[5]Co-first author
[6]Present address: Department of Genetics, St. Jude Children's Research Hospital, 262 Danny Thomas Place, Memphis, TN 38105, USA
*Correspondence: afsaneh.gaillard@univ-poitiers.fr (A.G.), pierre.vanderhaeghen@ulb.ac.be (P.V.)
http://dx.doi.org/10.1016/j.neuron.2015.02.001

SUMMARY

Pluripotent stem-cell-derived neurons constitute an attractive source for replacement therapies, but their utility remains unclear for cortical diseases. Here, we show that neurons of visual cortex identity, differentiated in vitro from mouse embryonic stem cells (ESCs), can be transplanted successfully following a lesion of the adult mouse visual cortex. Reestablishment of the damaged pathways included long-range and reciprocal axonal projections and synaptic connections with targets of the damaged cortex. Electrophysiological recordings revealed that some grafted neurons were functional and responsive to visual stimuli. No significant integration was observed following grafting of the same neurons in motor cortex, or transplantation of embryonic motor cortex in visual cortex, indicating that successful transplantation required a match in the areal identity of grafted and lesioned neurons. These findings demonstrate that transplantation of mouse ESC-derived neurons of appropriate cortical areal identity can contribute to the reconstruction of an adult damaged cortical circuit.

INTRODUCTION

Many neurological diseases strike the cerebral cortex, including stroke, epilepsy, and neurodegeneration. Despite its well-known plasticity, the adult cortex displays a poor ability to self-repair, whether by generating new cells or long-range connections (Gates et al., 2000).

Two main strategies have been proposed to induce or facilitate neural repair following cortical lesions: cell transplantation and recruitment or reprogramming of endogenous neural precursors (Arlotta and Berninger, 2014; Gates et al., 2000). Grafting in neonatal cortex has proved to be very efficient and has been widely used as a tool to study the mechanisms of specification of cortical neurons (Gaillard et al., 1998a; O'Leary and Sahara, 2008). As for grafting in the adult brain, initial attempts only documented a very limited axon outgrowth ability of grafted neurons (Guitet et al., 1994; Isacson et al., 1988; Sørensen et al., 1996b), suggesting that the adult brain was poorly permissive to allow axonal growth from embryonic cortical neurons. However, studies using more sensitive and specific tools to lesion the cortex and to trace the projections of the grafted cells have reported that grafted embryonic cortex neurons could display specific patterns of long-range projections, at least in some conditions (Fricker-Gates et al., 2002; Gaillard et al., 2007; Hernit-Grant and Macklis, 1996). Most strikingly, it was reported that grafted embryonic cortex neurons could effectively reestablish specific patterns of subcortical projections and synapses following cortical lesions (Gaillard et al., 2004, 2007).

While these studies open the possibility of cell transplantation for cortical repair, the very limited accessibility of human fetal cortical tissue constitutes a serious limitation to consider such approaches in a clinical setting. Given their greater accessibility and standard use, embryonic stem cells (ESCs) and induced pluripotent stem cells (iPSCs) hold great promise as a reliable source for cell replacement therapies (Aboody et al., 2011). Transplantation experiments using neural derivatives of ESCs have shown their promising capacity to integrate in the developing or adult brain and, in some cases, to promote functional recovery in experimental models of neurological diseases (Chiba et al., 2004; Friling et al., 2009; Kim et al., 2002; Kriks et al., 2011; Lamba et al., 2009; Ma et al., 2012; Roy et al., 2006; Tabar et al., 2005; Yang et al., 2008). Similar results were obtained with neural iPSC derivatives (Hargus et al., 2010; Wernig et al., 2008). Most of these studies have stressed the importance of the use of differentiated cells of desired regional identity, such as midbrain dopaminergic neurons for Parkinson disease, for instance.

We and others previously demonstrated the directed differentiation of cortical pyramidal/projection neurons from mouse and human ESCs (Anderson and Vanderhaeghen, 2014; Eiraku et al., 2008; Espuny-Camacho et al., 2013; Gaspard et al., 2008; Shi et al., 2012; van den Ameele et al., 2014; Vanderhaeghen, 2012). Using a chemically defined culture condition devoid of any added morphogen, we found that mouse ESCs spontaneously differentiate into cortical progenitors that further differentiate into pyramidal neuron subtypes corresponding to all six cortical layers. Notably, following grafting into mouse neonatal cortex, ESC-derived cortical neurons send projections that are strikingly similar to native cortical neurons, with a predominantly occipital (visual and limbic) areal identity (Gaspard et al., 2008, 2009b).

Here, we examined the capacity of mouse ESC-derived pyramidal neurons of specific areal identity to contribute to the repair of cortical lesions in adult mice. ESCs were differentiated into cortical neurons and progenitors of occipital identity and then grafted into lesioned adult mouse visual cortex. Grafted neurons established robust and specific long-range projections and synapses corresponding to visual circuits. Grafted neurons also received significant input from the visual thalamus and responded appropriately to visual stimuli in vivo, thus revealing their potential for functional restoration of cortex circuitry. Notably, grafting of the same neurons into the lesioned motor cortex, or of embryonic motor cortex neurons into the lesioned visual cortex, did not lead to similar reestablishment, indicating that it required a match in the areal identity of grafted neurons and lesioned cortex. These findings reveal areal specificity in the repair of the lesioned cerebral cortex following transplantation of ESC-derived pyramidal neurons and provide new insights for the future design of cell therapy enabling to rebuild cortical circuits in a highly specific way.

RESULTS

Transplanted ESC-Derived Cortical Neurons Integrate Successfully into Lesioned Adult Brain, with No Evidence of Host/Transplant Cell Fusion

In order to test the potential of ESC-derived cortical neurons for cortical repair, we used a well-established model of focal neurotoxic lesions of the cerebral cortex (Schwarcz et al., 1979) in adult mice, resulting in major neuronal and innervation loss (Figures S1A–S1D), focusing on the visual cortex. Mouse ESCs were first differentiated in vitro for 14 days following an intrinsic pathway of corticogenesis using a chemically defined medium containing cyclopamine (Gaspard et al., 2008, 2009a; Tiberi et al., 2012a). In these conditions, ESCs differentiated robustly into pyramidal neurons of all layer identities, but with mostly visual and limbic areal identities corresponding to occipital cortex, both at the level of gene expression in vitro (Figures S1E and S1G), and patterns of axonal projections following grafting into neonatal cortex (Gaspard et al., 2008). In order to track the identity and axonal projections of the grafted cells, we used a tau-GFP knockin ESC line where GFP is expressed under the control of the neuronal tau promoter (Gaspard et al., 2008). The ESC-derived cortical cells were grafted 3 days after the lesion in the same cortical site, and the identity and projections of the grafts were then monitored up to 12 months following grafting.

Analysis of the animals grafted with ESC-derived cortical neurons indicated that 67% of them (n = 47/70) contained a graft after 1 month; 70% (n = 21/30), after 3–4 months; and 61% (n = 8/13), after 12 months. The grafts were typically located in the cortex or in the underlying white matter and did not display any obvious cytoarchitecture (Figures 1A–1E). They consisted essentially of differentiated neurons (as assessed by expression of tau-GFP and microtubule-associated protein 2 [MAP2]), expressing markers of cortical pyramidal identity of distinct layers, and a minority of GABA-ergic neurons, similar to those observed following neonatal grafting (Gaspard et al., 2008) (Figure 1D; Figures S1H–S1K). Notably, most ESC-derived neurons also expressed the occipital cortex marker COUP-TFI (Figure S1F). The transplant also contained glial fibrillary acidic protein (GFAP)-positive astrocytes and IBA1-positive activated microglial cells, which were particularly abundant at the transplant-host border (Figures S1L–S1Q).

Host-transplant cell fusion was previously reported between ESC-derived cells and host neurons (Cusulin et al., 2012; Ying et al., 2002), while it was not observed with cells of embryonic cortex origin (Gaillard et al., 2007). In order to test whether cell fusion occurred in our experimental setting, tau-GFP ESC-derived cortical cells were differentiated and transplanted similarly but in transgenic mice expressing the tdTOMATO reporter ubiquitously (Madisen et al., 2010) (n = 8). Systematic inspection of the transplant and its borders with the host failed to reveal any double-labeled cells (Figures S2A–S2I), indicating that cell fusion appears to be absent or negligible in our experimental setting. Notably, the majority of the MAP2-positive neurons were GFP positive and tdTOMATO negative (98.6%; 157.1 ± 53), while only 1.39% (2.1 ± 0.56) of MAP2-positive neurons were tdTOMATO positive and GFP negative (n = 2,119 neurons counted in four transplanted animals; 529.7 ± 176.3 is the average of neurons counted per animal ± SEM). In addition, this approach revealed host-derived cells within the transplant, corresponding mostly to blood vessels and microglia, while most of the astrocytes and neurons found in the transplant were of ESC origin (Figures S2J–S2U). In a few cases (6/47), the graft also contained a large amount of non-neural cells (negative for nestin or GFP, with morphology reminiscent of fibroblast-like cells), which might reflect teratoma formation from remaining undifferentiated ESCs (data not shown). In these cases, very few axonal projections were observed to subcortical targets. This clearly differs from what we observed following grafting in parallel of the same differentiated cells into neonatal brain, where the grafts showed signs of teratoma-like formation in much lower frequency (Gaspard et al., 2008). This could reflect the fact that the neonatal brain may constitute a better environment for neural differentiation (Friling et al., 2009; Wernig et al., 2008).

Progressive Axonal Outgrowth of Transplanted ESC-Derived Cortical Neurons

We next focused on potential axonal projections from the transplants (Figures 1E–1K). Inspection of the brains containing a graft 1 month after grafting revealed, in 40% of the cases (n = 17/47), far-reaching graft-derived GFP+ axonal growth, following specific paths (corpus callosum, internal and external capsule, cerebral peduncles) and reaching specific targets of endogenous cortical neurons that would correspond to all layer identities,

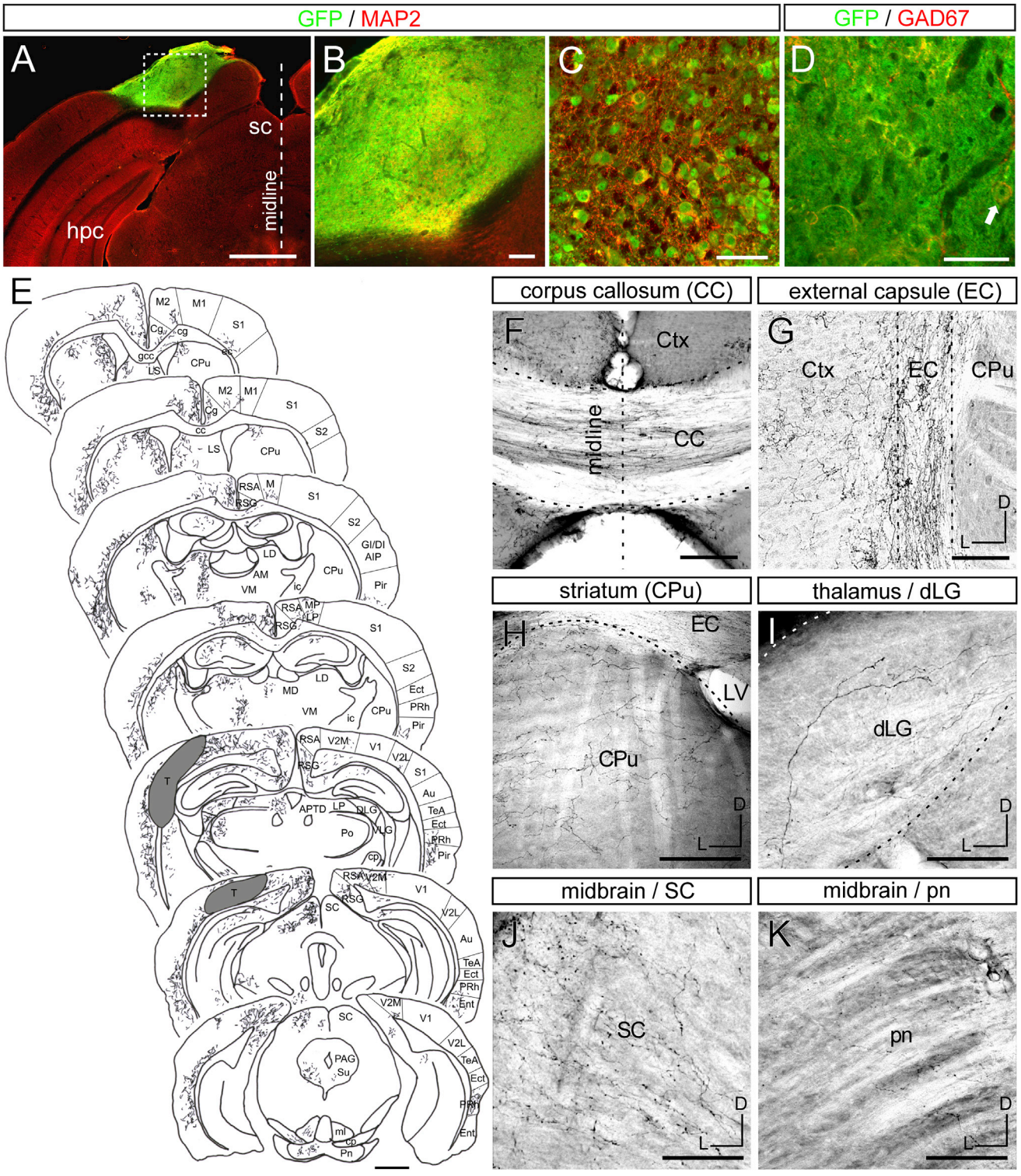

Figure 1. ESC-Derived Cortical Neurons Send Widespread, but Specific, Projections following Grafting in the Lesioned Visual Cortex

(A–C) Illustrative case of a graft in the ibotenic-acid-lesioned visual cortex displaying GFP (green) and MAP2 (red) immunoreactivity. (B) corresponds to the inset in (A), and (C) shows the graft in high magnification. hpc, hippocampus.

(D) Few of the grafted neurons are GABAergic (GAD67) (arrow).

(legend continued on next page)

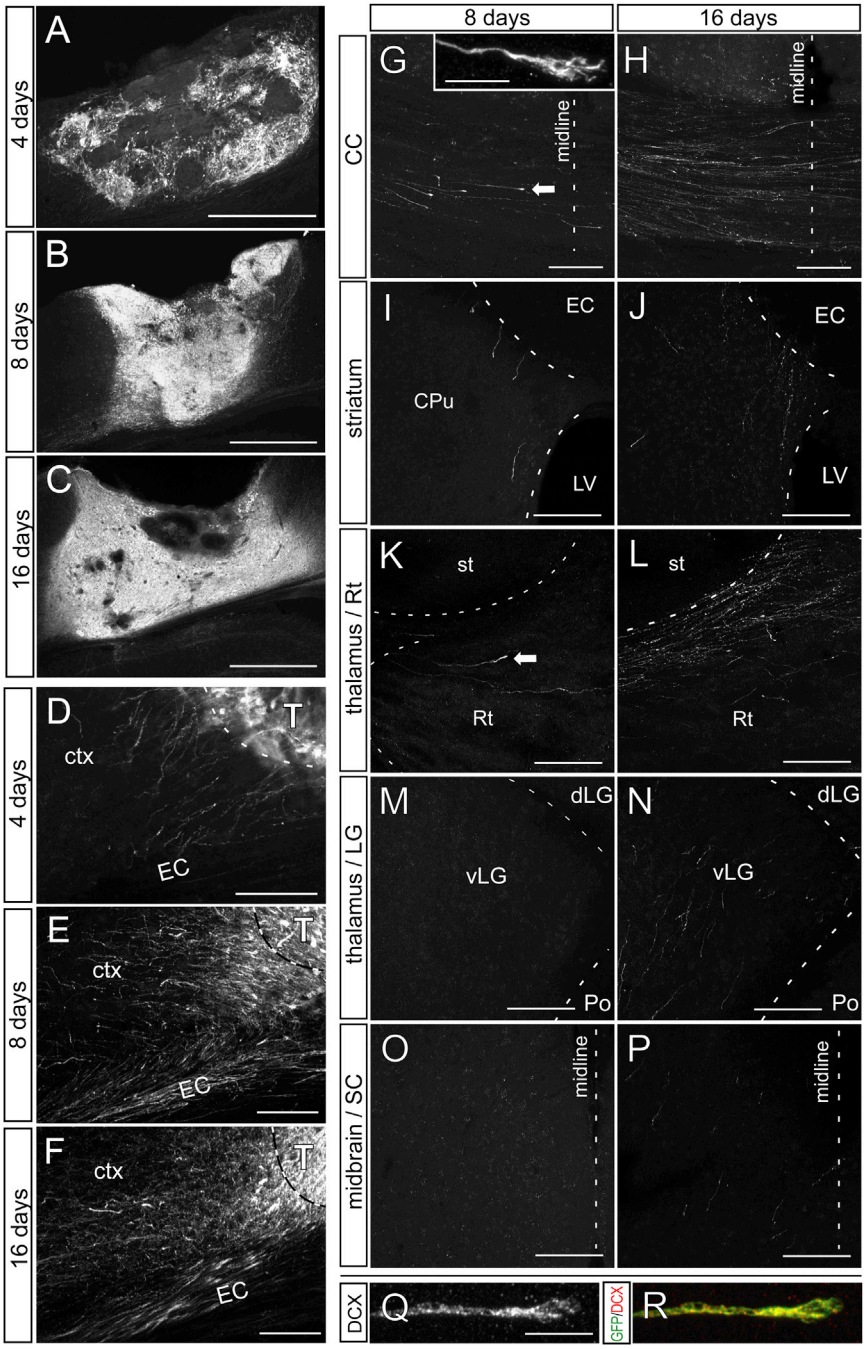

Figure 2. Projections from ESC-Derived Cortical Neurons Develop Progressively over Time following Grafting in the Lesioned Visual Cortex

(A–C) Representative grafts 4, 8, and 16 days after grafting.

(D–F) GFP+ fibers exit the graft after 4, 8, and 16 days. ctx, cortex; T, transplant.

(G–P) Projections in the (G and H) corpus callosum (CC); (I and J) striatum (st); (K and L) reticulate thalamus (Rt); (M and N) lateral geniculate nucleus of the thalamus (LG); and (O and P) SC of the midbrain 8 and 16 days after grafting. Fibers are absent in (M) LG and (O) SC after 8 days. Arrows show growth cones. The inset in (G) shows a growth cone in the CC. CPu, striatum caudate putamen; EC, external capsule; LV, lateral ventricle; vLG, ventral-lateral geniculate nucleus; Po, posterior nucleus; SC, superior colliculus.

(Q and R) Growth cone stained with doublecortin (DCX) and GFP.

Scale bars, 500 μm in (A)–(C); 100 μm in (D)–(F); 50 μm in (G)–(P); and 10 μm in (Q), (R), and (G, inset).

including ipsi- and contralateral (CL) cortex (layers II/III/V) and subcortical structures such as the striatum (layer V), thalamus (layer VI), and midbrain/hindbrain nuclei (layer V). These data indicate that ESC-derived neurons can integrate successfully into the lesioned adult cortex and can send long-range axons in a pattern similar to that of endogenous cortical neurons. In order to gain insight into the developmental course of axonal projections, we performed a time-course analysis, from 4 to 90 days following transplantation (Figure 2; Figure 3). This revealed a progressive neuronal differentiation (Figures 2A–2C) and axonal outgrowth (Figures 2D–2P and 3) until 1 month post-transplantation. At 4 days following transplantation, only a few GFP+ axons could be detected, all in the close vicinity of the transplant (none further than 250 μm) (Figure 2D). At 8 days post-transplantation, GFP-positive axonal fibers extended further to the external and internal capsule, as well as the corpus callosum (Figure 2). Single fibers entered the thalamus through the reticular nucleus, while no fibers could be detected in the rest of the thalamus or other subcortical targets. At 16 days post-transplantation, axonal growth had become more profuse and reached thalamic and midbrain nuclei (Figure 2), but the level of axonal density was much lower than what was observed after 1 month (Figure 3). In addition, at early stages (before 1 month),

(E–K) GFP+ axons detected by immunohistochemistry after 3–4 months in various tracts and targets of the host brain. (E) Camera lucida drawing showing an overview of the transplant (T) and its derived projections 4 months after grafting in the visual cortex. (F) corpus callosum (CC); (G) external capsule (EC); (H) striatum caudate putamen (CPu); (I) dLG; (J) SC; and (K) pontine nucleus (pn). Dorsal (D) is up and lateral (L) is at left in (G–K). Scale bars, 1 mm in (A and E), 100 μm in (B and F–K), and 50 μm in (C and D).

See also Figures S1 and S2.

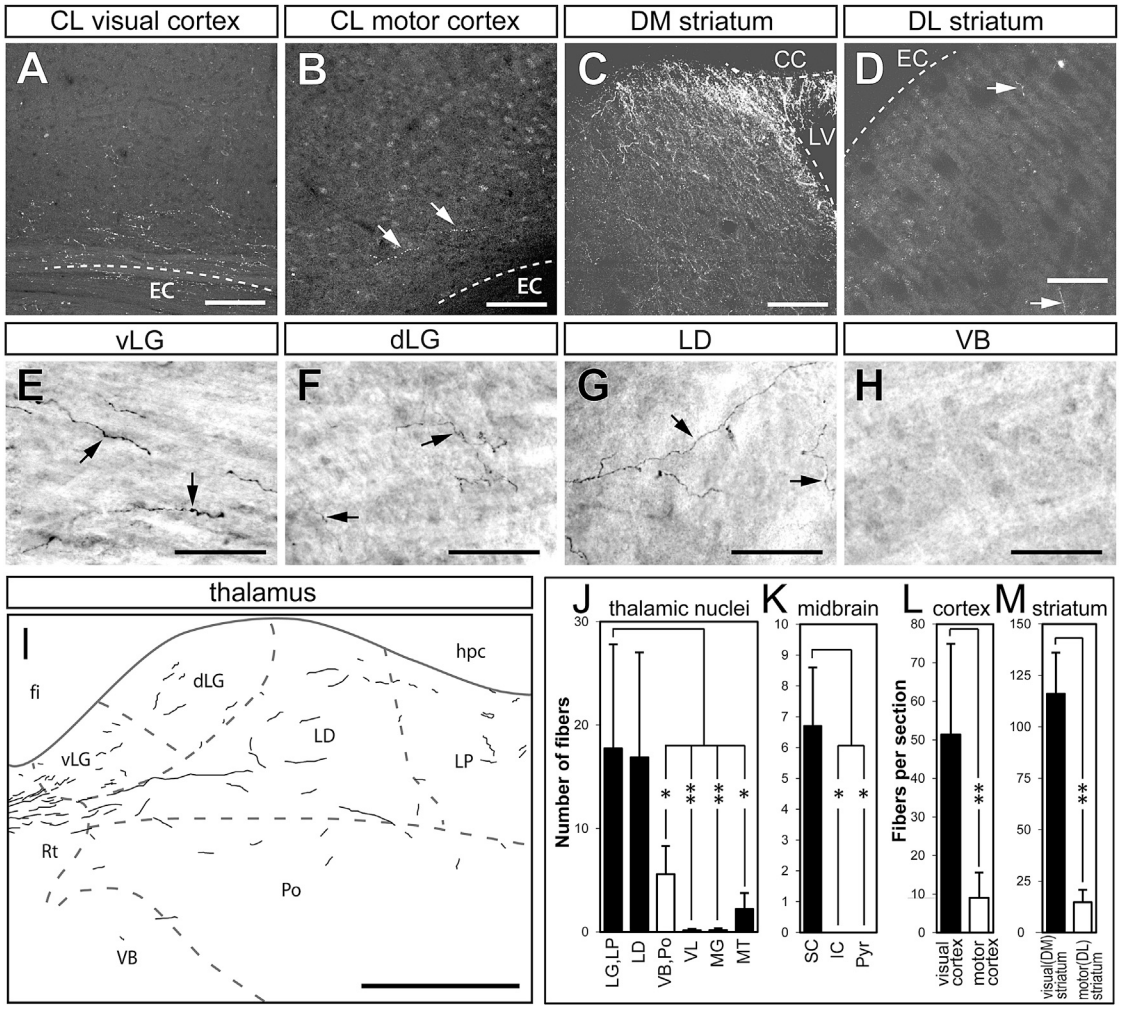

Figure 3. ESC-Derived Cortical Neurons Send Projections Preferentially to Targets of the Visual Cortex, 1 Month after Grafting

(A–I) Distribution of graft-derived GFP+ fibers in (A and B) CL cortex, (C and D) ipsilateral striatum, or (E–I) thalamic nuclei, following grafting in the visual cortex, detected by GFP immunofluorescence in (A)–(D) or immunohistochemistry in (E)–(H). (I) Camera lucida drawing showing an overview of graft-derived projections in the thalamus. The abundance of GFP+ fibers was higher (A and B) in visual cortex than in motor cortex, (C and D) in DM striatum than in DL striatum, and (E–I) in the visual and/or limbic thalamic nuclei vLG, dLG, LD, and LP than in the somatosensory thalamic nuclei VB and Po.

(J–M) Quantification of GFP+ fibers in the (J) thalamic nuclei, (K) midbrain, (L) CL cortex, and (M) DM and DL striata.

CC, corpus callosum; LV, lateral ventricle; vLG, ventral-lateral geniculate nucleus; LD, laterodorsal nucleus; LP, lateral posterior nucleus; VB, ventrobasal nucleus; Po, posterior nucleus; Rt, reticular area; fi, fimbria; hpc, hippocampus; IC, inferior colliculus; Pyr, pyramidal tract; LG, lateral geniculate nucleus; MG, medial geniculate nucleus; MT, medial thalamus.

Values are expressed as the mean ± SEM. Scale bars, 100 μm in (A)–(D), 50 μm in (E)–(H), and 500 μm in (L). *$p < 0.05$; **$p < 0.01$.

See also Figure S3.

GFP-positive axonal tips displayed the morphology of typical growth cones and expressed the DCX marker of immature neurons (Figures 2G, 2K, 2Q, and 2R). After 3–4 and 12 months, the distribution of fibers remained similar to that after 1 month (Figures 1 and 3). For most subsequent analyses, the brains were analyzed 1 and 3 months after grafting.

ESC-Derived Cortical Neurons Grafted into Lesioned Visual Cortex Send Long-Range Axonal Projections of Specific Areal and Layer Identity

Next, we examined in more detail the specificity of the axonal projections from the grafted neurons 1 month after transplantation (Figure 3). Remarkably, we found that graft-derived projections preferentially reached cortical and subcortical structures which, in the intact brain, receive projections from the visual and, to a lesser extent, the limbic cortex. These included projections to the visual cortex (V1/V2) CL to the graft, while very few fibers were found in the CL motor (M1) or somatosensory (S1) areas (Figures 3A, 3B, and 3L). Similarly, GFP+ axons were found preferentially in the dorso-medial (DM) striatum, which receives mainly input from the visual cortex, while very few fibers were found in its dorso-lateral (DL) part, a main target of the motor cortex (Figures 3C, 3D, and 3M). In the thalamus, fibers were found throughout primarily visual and limbic thalamic nuclei, while

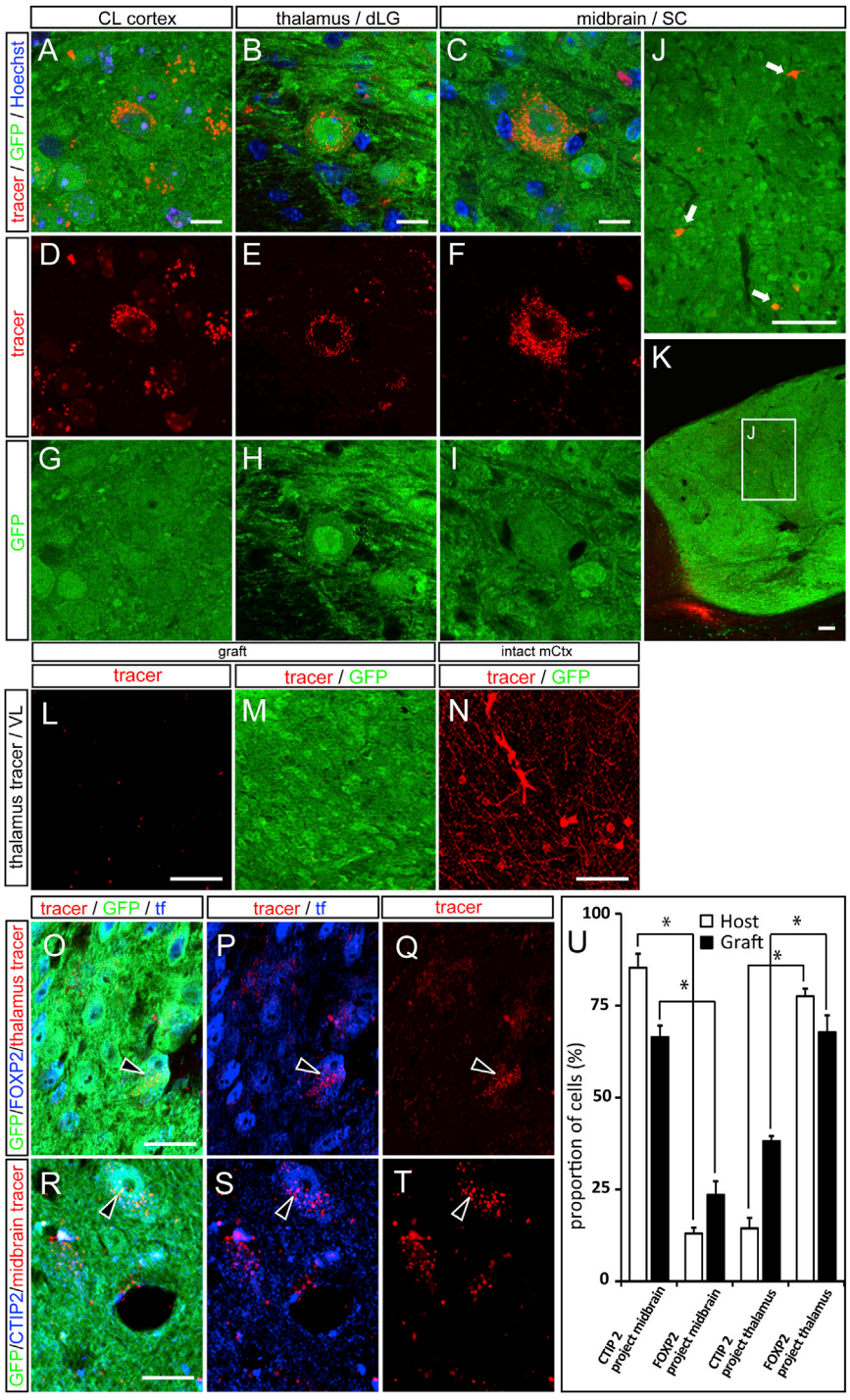

Figure 4. Tracer Injections into Visual Cortex Targets Label Retrogradely ESC-Derived GFP+ Neurons Inside the Graft

(A–K) Retrograde BDA labeling is present in the soma of grafted neurons upon tracer injections into (A, D, and G) the CL visual cortex (CL cortex), (B, E, and H) the thalamic dLG nucleus, and (C, F, and I–K) the SC of the midbrain. Low-magnification images of the SC retrograde tracing show the localization of retrogradely labeled GFP+ neurons in the inner part of the graft (inset, J and K).

(L–N) Absence of retrogradely labeled neurons within the graft following injections of retrograde tracer into the thalamic VL, while, at the same time, there is ample BDA labeling in the motor cortex.

(O–Q) Thalamic injection of a retrograde tracer (red) labels FOXP2 (blue) and GFP (green) double-positive grafted neurons. Arrowheads show grafted neurons positive for GFP/FOXP2 and the retrograde tracer. tf, transcription factor.

(R–T) SC (midbrain) injection of a retrograde tracer (red) labels CTIP2 (blue) and GFP (green) double-positive grafted neurons. Arrowheads show grafted neurons positive for GFP/CTIP2 and the retrograde tracer.

(U) Quantification of the percentage of Ctip2- or FOXP2-positive grafted cells labeled with the midbrain or the thalamic retrograde tracer. Values are expressed as the means ± SEM. *$p < 0.05$. Scale bars, 10 μm in (A)–(C) and (O)–(T), 100 μm in (J) and (K), and 25 μm in (L)–(N).

See also Figure S4.

almost none were detected in motor, S1, or auditory system nuclei (Figures 3E–3J). Finally, within the midbrain/hindbrain, projections were found almost exclusively in the superior colliculus (SC), pontine nucleus, raphe nuclei, and periaqueductal gray matter, which receive their main projections from the visual and limbic cortex, while no projections were found in the inferior colliculus or pyramidal tract, even 4 months after grafting (Figures 1E–1K). Notably, these patterns corresponded to those obtained following grafting of the native embryonic occipital cortex into similarly lesioned visual cortex (Figure S3), confirming that the pattern observed indeed corresponds to the expected intrinsic identity of the grafted cells.

To determine independently the extent of the observed cortico-cortical and subcortical projections, we performed retrograde labeling experiments in transplanted animals 3–9 months after grafting, targeting the CL visual cortex (n = 10 animals), thalamus (lateral geniculate nucleus) (n = 11), midbrain (SC) (n = 9), and the motor thalamic ventrolateral nucleus (VL) (n = 2) (Figure 4; Figure S4). This revealed clear patterns of retrograde labeling from the thalamic DL geniculate nucleus (dLG) and SC in the host cortex (Figures S4A–S4F) and among GFP+ neurons (Figures 4A–4K) in most injected mice that had a graft (7/10 for CL cortex, 6/11 for thalamus, and 6/9 for SC), while no retrograde labeling could be detected following injections in VL (Figures 4L–4N). Notably, the labeled neurons could be found not only at the border but also within the depth of the transplant (Figures 4J and 4K).

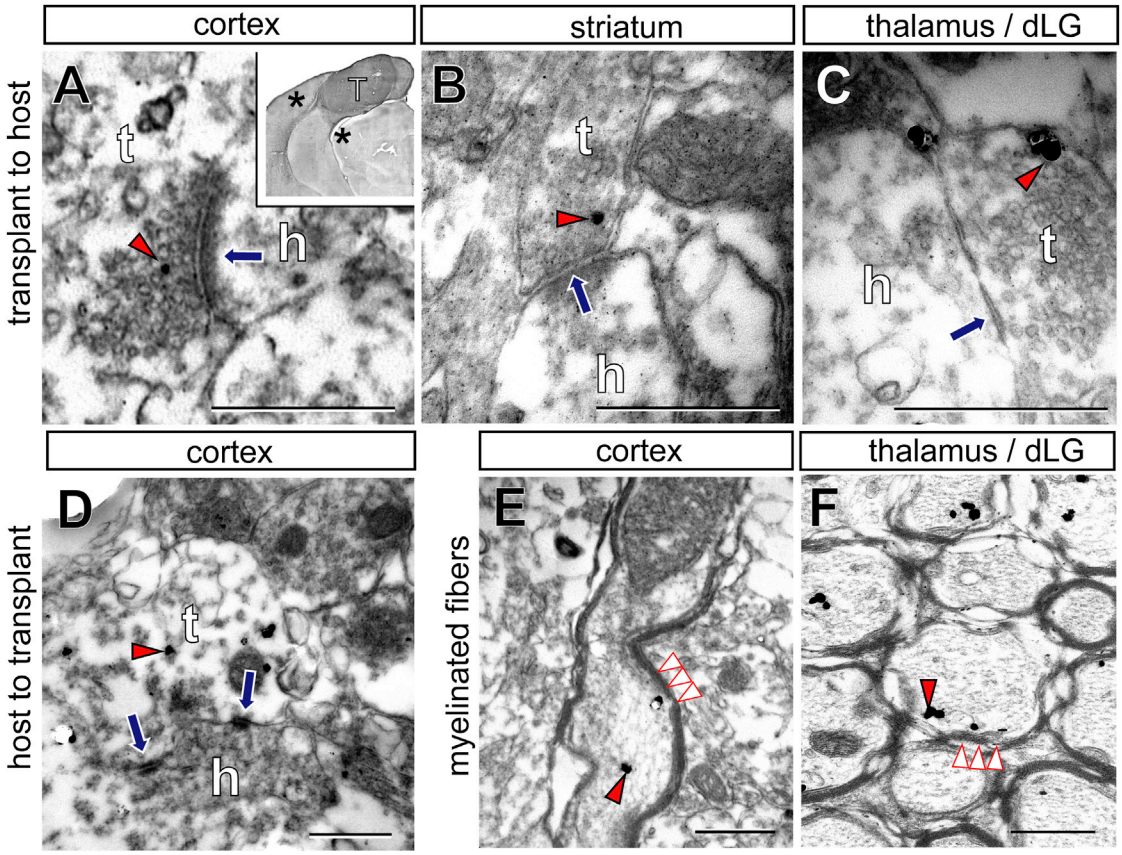

Figure 5. Synaptic Contacts between the Transplant and the Host Assessed by Electron Microscopy 3–4 Months after Transplantation

(A–F) Transplant (t)-to-host (h) contacts in the (A) cortex, (B) striatum, and (C) dLG and (D) host-to-transplant contacts in the cortex. Myelin sheets surrounding the GFP+ fibers were observed in the (E) cortex and (F) dLG. Red arrowheads indicate immunogold labeling for GFP, blue arrows indicate synapses (the arrows being on the post-synaptic side), and white arrowheads indicate myelin sheets. Inset in (A) shows the location of the electron microscopy pictures (indicated by asterisks) in relation to the transplant. Scale bars, 100 nm in (A)–(C) and 500 nm in (D)–(F).

Overall, these data indicate that ESC-derived transplants send axonal projections to subcortical targets in a way that is qualitatively similar to that in the visual cortex. In order to compare the transplant-derived projections with those of the host in a quantitative manner, we analyzed further a set of transplanted animals that had undergone smaller lesions of the visual cortex, so that the spared visual cortex could be directly compared with the transplanted neurons (Figures S4G–S4T). In addition, transplantations of embryonic motor cortex were performed in the lesioned visual cortex as a control of specificity. This quantitative analysis revealed that the density of transplanted ESC neurons labeled from dLG was 29% of the density of labeled host neurons of the visual cortex labeled from dLG, while no labeled neurons were detected following transplantation of the embryonic motor cortex (Figures S4G–S4M). Similarly, the density of transplanted ESC-derived neurons labeled from SC was 27%, compared to the density of host neurons of the visual cortex labeled from SC, while no labeled neurons were detected following transplantation of embryonic motor cortex (Figures S4N–S4T) (n = 4 animals for each condition).

In order to further relate axonal output of the transplanted neurons to host-derived projections, we combined retrograde labeling with staining for layer-specific markers. This revealed that the majority of neurons retrogradely labeled from the midbrain were labeled with CTIP2, a layer V marker, while the majority of neurons retrogradely labeled from the thalamus expressed FoxP2, a marker of layer VI neurons. These data indicate that the transplanted neurons display layer-specific patterns of projection in accordance with their molecular identity, like native host neurons of the visual cortex (Figures 4O–4U).

Reciprocal Connectivity between the Grafted Neurons and the Host Brain

The establishment of functional neuronal circuits requires not only axonal projections but also synapses. To test whether the grafted ESC-derived cortical neurons were capable of forming synapses with the host, we then examined grafted brains using electron microscopy combined with GFP immunogold labeling (Gaillard et al., 2007). After 1 month post-transplantation, no synapses were detected, but 3–4 months after grafting, GFP-labeled terminals developed synapses with host neurons of the cortex and subcortical targets (Figures 5A–5C), and conversely, host neurons were found to establish synaptic contacts with the grafted GFP+ neurons (Figure 5D). GFP-labeled fibers also

displayed myelination by the host, including in long-range subcortical targets (Figures 5E and 5F). In addition, in order to test whether the graft received long-range projections from the host brain, we performed anterograde tracer injections in transplanted animals 3–9 months after grafting, into the dLG of the thalamus (n = 7 animals) (Figures 6A–6E) and CL visual cortex (n = 6) (Figures 6F–6K) of grafted animals. This revealed labeled fibers inside the graft in the visual cortex in most of the cases examined (thalamus: 6/7; cortex: 5/6), indicating that the transplant is indeed innervated by the host visual thalamus and CL visual cortex (Figure 6). In order to relate this input to the host cortex in a more quantitative manner, we performed anterograde tracing and transplantations following small lesions of the visual cortex, where spared host and transplant could be directly compared. This revealed that the density of fibers found in the ESC-derived transplant was 18.1% of the labeling found in the intact host, while the anterograde labeling in the transplants derived from embryonic motor cortex was 3.8% of that in the intact host (Figures 6L–6R).

Altogether, these data suggest that ESC-derived cortical neurons not only send axonal projections but also can significantly integrate into existing cortical circuits, thus providing a potential substrate for their functional repair.

Some Grafted ESC-Derived Cortical Neurons Are Electrophysiologically Similar to Visual Cortical Neurons and Can Respond to Visual Stimuli In Vivo

To assess the functionality of the grafts, we performed extracellular recordings in vivo in the visual cortex of control mice (n = 6) and in grafts of mice that previously underwent ibotenic-acid-induced lesions of the visual cortex (n = 5). We also recorded from mice (n = 5) that were lesioned by partial aspiration of the visual cortex, resulting in more severe disruption of thalamocortical projections to the lesioned area (Sørensen et al., 1996a), in order to test more stringently the impact of ESC-derived neurons on cortical repair. Notably, a similar rate of successful integration and visual-like pattern of axonal outgrowth were obtained in these mice (Figure S5A; data not shown).

Recordings were performed 3–9 months after grafting in both lesioning conditions. In order to identify the recorded neurons, juxtacellular neurobiotin injections were performed after the recordings. Extracellular recordings are always associated with inherent uncertainty about the identity of the recorded neurons. Therefore, only neurons that exhibited neurobiotin and GFP co-localization (Figures 7A–7C) were considered as grafted neurons, and their action potential (AP) waveform was specifically analyzed to confirm that electrophysiological recordings corresponded to single cells (Figures 7D and 7G). Finally, and most important to note, as a more stringent control for the identity of the recorded neurons, recordings were performed also in tdTOMATO transgenic mice to allow the identification of host-derived neurons. This confirmed that no host neurons could be found in the vicinity of the recorded neurons and that the few detected tdTOMATO cells all corresponded to blood vessels (Figures 7B and 7C).

Electrophysiological properties of recorded neurons (AP duration and frequency) were measured during a 1-min baseline period (Figures 7J and 7K). AP duration was similar between control neurons of unlesioned visual cortex and grafted ESC neurons following ibotenic acid or aspiration lesions (0.56 ± 0.04 ms, n = 12; 0.48 ± 0.03 ms, n = 7; and 0.64 ± 0.06, n = 10, respectively). No statistical difference in spontaneous AP firing frequencies was observed between the neurons recorded in control visual cortex and the grafted neurons (1.67 ± 0.32 Hz, n = 12; 1.12 ± 0.17 Hz, n = 7; 1.40 ± 0.41 Hz, n = 10, respectively). These results suggest that ESC-derived cortical neurons grafted into the lesioned visual cortex exhibit electrophysiological properties similar to those of native neurons of unlesioned visual cortex.

In order to assess the potential of grafted ESC-derived cortical neurons for specific repair of the visual cortex, we then examined more directly their function in vivo by testing whether they could be responsive to visual stimuli, as intact visual cortex would be. A 1-s light flash was used as a visual stimulus. In control unlesioned mice, 8 of 12 neurons recorded in the visual cortex exhibited an increase in their AP frequency in response to the light stimulus (Figure 7L), in accordance with published data (Cang et al., 2005; Niell and Stryker, 2008). Remarkably, a similar responsiveness to light was observed in most of the neurons recorded in the ESC-derived transplants following visual cortex lesions whether with ibotenic acid or aspiration (four of seven following ibotenic acid lesions, and six of ten following aspiration lesions) (Figures 7E, 7F, 7H, 7I, and 7L; Table S1).

Further analyses of the firing patterns of the neurons that responded to visual stimulus confirmed the robustness of the functional responsiveness of the grafted neurons. The light stimulation induced a strong increase in AP frequency (two-way ANOVA, $F[1, 15] = 32.55$, $p < 0.0001$) in control neurons (from 1.0 ± 0.65 to 22.00 ± 5.07 Hz), as well as in neurons from the transplants following ibotenic acid (from 1.09 ± 0.69 to 27.05 ± 8.89 Hz) and aspiration (from 1.67 ± 1.31 to 27.67 ± 8.46 Hz) lesions (Figure 7L). Altogether, these data indicate that at least some transplanted ESC-derived cortical neurons display functional properties similar to those of intact visual cortex, including responsiveness to light stimulation.

Areal Identity of the Transplant and the Damaged Cortex Must Match to Allow Successful Reestablishment of Cortical Projections

In general, these data suggest that ESC-derived cortical neurons are able to reestablish damaged neuronal pathways when their identity corresponds to the lesioned area. Alternatively, the ESC-derived neurons may be influenced by the surrounding host tissue and replace the missing projections in a non-specific way, regardless of their identity or of the location of the lesioned area.

In order to investigate these possibilities, we compared the axonal growth and targeting patterns obtained in animals lesioned and grafted in the visual cortex with those obtained following lesioning and grafting within the motor cortex. Indeed, following lesioning of the motor cortex, previous work has shown that the damaged projections can be reestablished following grafting of motor, but not visual, embryonic cortical tissue (Gaillard et al., 2007).

The survival and integration rate of the grafts in the lesioned motor cortex was roughly similar (with 29/47 grafted mice that

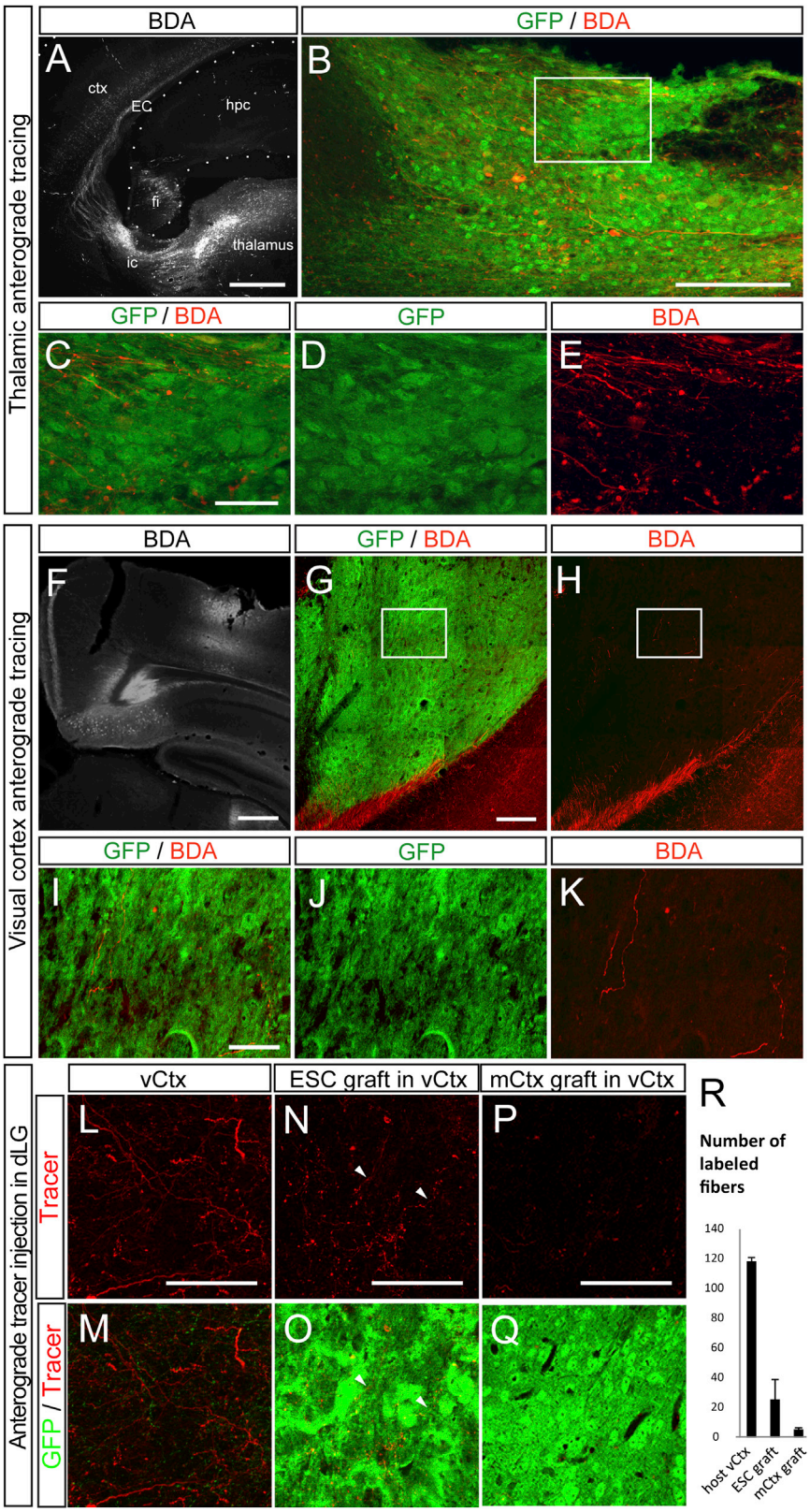

Figure 6. Host Input into the Graft Revealed by Anterograde Tracing 3–9 Months after Grafting

(A) Overview of the injection site in the thalamus and the BDA+ fibers (white) passing via the internal capsule (ic) to the external capsule (EC) and the cortex (ctx). hpc, hippocampus; fi, fimbria.

(B) Thalamic BDA+ fibers (red) in the ESC-derived graft (green).

(C–E) Detail of the BDA+ fibers in the inset in (B).

(F) Overview of the injection site in the CL visual cortex.

(G and H) Presence of BDA-labeled fibers inside the graft.

(I–K) Detail of the BDA+ fibers in the inset in (G) and (H).

(L–Q) Anterograde tracer injection in the dLG results in the presence of labeled fibers in the host adjacent visual cortex (vCtx) (L and M), as well as in ESC-derived grafts (N and O), but no labeling in the graft of motor cortex (mCtx) (P and Q).

(R) Quantification of number of labeled fibers.

Values are expressed as the mean ± SEM. Scale bars, 1 mm in (A), 200 μm in (B), 50 μm in (C) and (G), 500 μm in (F), 10 μm in (I), and 100 μm in (L)–(P).

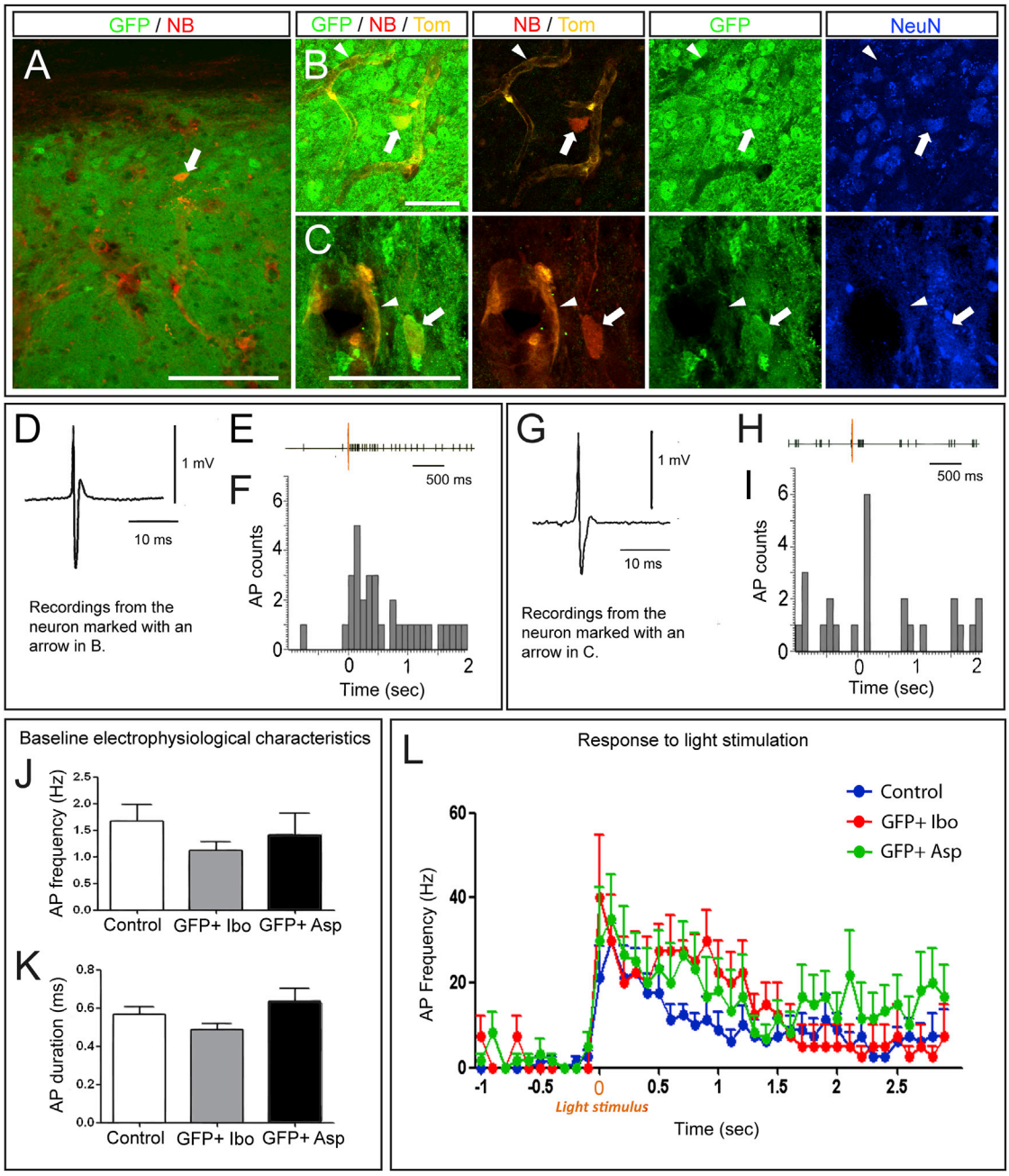

Figure 7. Electrophysiological Properties of Grafted Neurons after Visual Cortex Lesioning

(A–C) Identification of the neurons recorded within the transplant using immunofluorescence. The high-magnification images (B and C) illustrate that the Neurobiotin (NB, red)-labeled recorded neurons (for which tracings are displayed in D–G) are GFP positive (green), NeuN positive (blue), and negative for tdTOMATO (Tom, orange). The arrows in (B) and (C) point to the neurons for which the tracings are shown in (D)–(F) and (G)–(I), respectively. The arrowheads point to dTomato-positive non-neural cells (blood vessels).

(D–I) In (D) and (G), typical AP is shown for the neurons recorded in grafted GFP+ neuron in aspiration-lesioned cortex displayed in (B) and (C). (E–F and H–I) Representative light-induced changes in AP firing rates in the transplanted neurons shown in (B) and (C). The traces on top represent the typical raster plots, and the yellow line represents the initiation of light stimulation. The peristimulus histogram represents AP count per bin before and after visual stimulation. sec, seconds.

(J and K) Baseline electrophysiological characteristics, i.e., (J) frequency and (K) duration of AP in unlesioned (control) mouse visual cortex, grafted GFP+ neurons in ibotenic-acid-lesioned cortex (Ibo), and grafted GFP+ neurons in aspiration-lesioned cortex (Asp).

(L) Histogram showing the firing frequency (mean ± SEM) in response to a light stimulus in all neurons recorded in each experimental condition.

Values are expressed as the mean ± SEM. Scale bars, 100 μm in (A) and 20 μm in (B) and (C).

See also Figure S5 and Table S1.

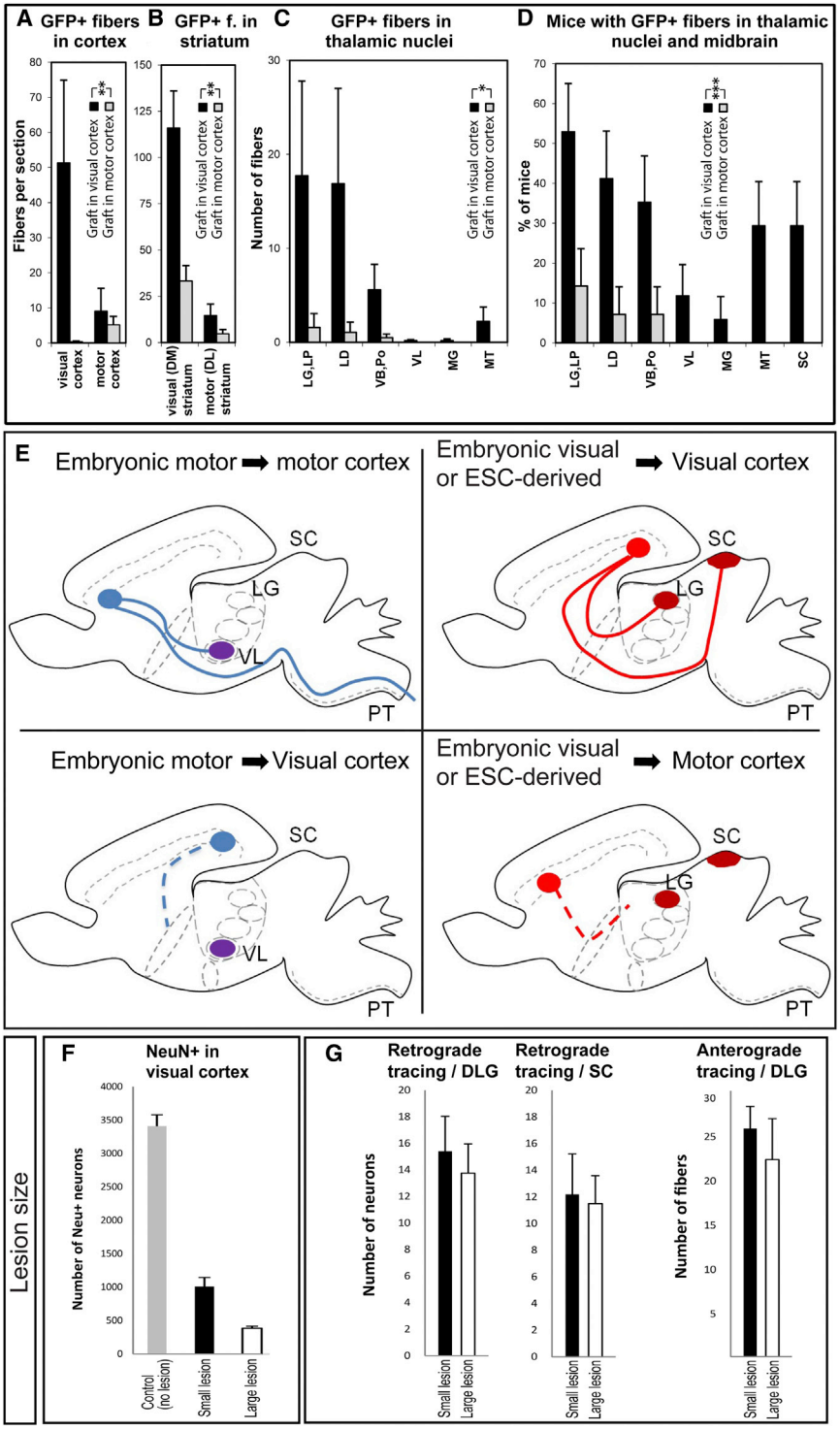

Figure 8. Distribution of Graft-Derived Axonal Projections following Grafting into Ibotenic-Acid-Lesioned Visual Cortex versus Motor Cortex

(A–C) Quantification of GFP+ fibers (f) in (A) visual and motor cortex and (B) in DM and DL striatum of all mice with subcortical projections. (C) Quantification of GFP+ fibers in thalamic nuclei of all mice with subcortical projections. LG, lateral geniculate nucleus; LP, lateroposterior nucleus; LD, laterodorsal nucleus; VB, ventrobasal nucleus; Po, posterior nucleus; MG, medial geniculate nucleus; MT, medial thalamus.

(D) Proportion of cases with GFP+ fibers in thalamic nuclei and the midbrain.

(E) Schematic illustration of the pattern of graft-derived subcortical projections, in motor-specific (VL, PT) and visual-specific (dLG, SC) targets following the grafting of embryonic motor cortex (left panels) or embryonic visual cortex/ESC-derived cortical neurons (right panels) into adult motor cortex (upper left, lower right) or adult visual cortex (lower left, upper right).

(F) Quantification of the number of NeuN+ neurons remaining in the visual cortex following small or large lesions.

(G) Quantification of the number of tracer-labeled neurons and fibers following retrograde and anterograde tracer injections, respectively. PT, pyramidal tract.

Values are expressed as the mean ± SEM. *p < 0.05; **p < 0.01; ***p < 0.001.

See also Figures S6–S8.

contained a graft after 1 month) to that of the grafts in the lesioned visual cortex. However, the pattern of projections observed was remarkably different (Figures 8A–8E; Figure S6). Indeed, far fewer projections could be observed in the cortex and striatum, almost none in the thalamus, and none in the midbrain/hindbrain, whether looking at targets of the motor or visual cortex (Figures 8A–8D; Figures S6A–S6E).

Conversely, we examined whether ESC-derived neurons transplanted in the motor cortex received any significant input from the host brain. Anterograde tracing from dLG or VL failed to reveal any significant pattern of projections (Figures S6F–S6I). We then looked for signs of functional integration using extracellular recording of the transplanted neurons. While we could successfully record the basal activity of neurons in the ESC-derived transplants in the lesioned motor cortex, no increase in firing rate could be detected in response to light stimuli (Figures S5D, S5E, S5H, and S5I).

On the other hand, we performed grafting of embryonic motor cortex tissue, (collected at embryonic day (E)14 (n = 9 transplanted animals) or E16 (n = 5), into the lesioned visual cortex (Figures S7A and S7B). Notably, in this case, despite successful survival and integration of the transplant, we could not detect any GFP-positive projections to subcortical targets (Figures S7A–S7E), which was confirmed with retrograde tracing

from dLG or SC (Figures S4K–S4M and S4R–S4T). In addition, we examined the thalamocortical input to these transplants using anterograde tracing from dLG and VL, which failed to reveal any significant projections (Figures 6P–6R, S7F, and S7G). The presence of functional input from the host was further tested using extracellular recording in the same transplantation paradigm, but it failed to reveal any light responsiveness in the transplanted neurons (Figures S5B, S5C, S5H, and S5I). Altogether, these data strongly suggest that the patterns of output, input, and functional integration observed following transplantation of ESC-derived neurons depend mostly on the correspondence of identity between the transplanted cells and the lesioned cortex, so that the successful reestablishment of the damaged cortical projections requires a strict identity match between the grafted neurons and the lesioned area (Figure 8E).

Successful Integration of the Transplant Requires a Cortical Lesion, but Is Not Greatly Influenced by the Number of Remaining Unlesioned Host Neurons

Next, we tested whether and how much the lesion contributes to the pattern of integration of the transplanted neurons. As a first control, ESC-derived neurons were transplanted in the visual cortex of animals that had not undergone any prior lesion. In these cases, while a graft was present in all cases examined (n = 3/3), no axonal projections were observed except in the immediate vicinity of the graft (data not shown), as previously shown for transplantation of embryonic cortical tissue (Gaillard and Jaber, 2007). Then, we determined the extent to which the removal of the host's source or target cells in the primary visual cortex contributes to the ability of the graft to make and receive connections with the host. Specifically, we compared the output and input of projections in animals that underwent distinct ranges of lesions before transplantation (using different amounts of ibotenic acid), i.e., large lesions that left 11.42% of the NeuN+ neurons in V1 and smaller lesions that left 28.57% of NeuN+ neurons (n = 4 mice per group) (Figure 8F). Next, we determined the levels of axonal projections from and to the transplant using GFP labeling and anterograde and retrograde tracings. This revealed comparable levels of GFP-labeled axonal projections in small or large lesions (Figures 8A–8C and S8A), which was confirmed by quantification of neurons retrogradely labeled from dLG or SC (Figures 8G and S8B–S8I). Conversely, the levels of thalamocortical projections, assessed by dLG anterograde labeling, appeared to be similar in the grafts following small or large lesions (Figures 8G and S8J–S8M) (n = 4 mice per group).

These data indicate, overall, that successful transplantation requires lesioning of the brain but that the amount of remaining host neurons does not appear to have a detectable impact on the level of output and input of the transplanted neurons.

DISCUSSION

Neurological diseases frequently involve cortical lesions, many of which could benefit, in principle, from cell therapy strategies for brain repair. Here, we examined whether cortical projection neurons obtained by directed differentiation from mouse ESC could contribute to the reestablishment of cortical circuits following a lesion in the adult brain. Our data demonstrate, for the first time, that ESC-derived cortical neurons can establish modality-specific patterns of anatomical and functional connectivity within the adult brain following a cortical lesion, which constitutes an important step toward the rational use of pluripotent stem-cell-derived neurons in brain repair strategies targeting the cortex.

Notably, we tested specifically for cell fusion events in our experimental setting, since it was previously reported for ESC-derived neural progenitors and host cortical neurons (Cusulin et al., 2012). The absence of any direct evidence for cell fusion events in tdTomato-expressing mice, together with the gradual temporal pattern of neuronal differentiation, axonal outgrowth, and synaptogenesis, collectively rule out the possibility that cell fusion could contribute to our findings in any significant way.

A major challenge for brain repair is to reestablish specific and complex patterns of neuronal connectivity. As for the cortex, this means to generate specific patterns of cortical layer and areal identity in order to rebuild functional circuits in a physiological way, even though recovery may also benefit from transplanted cells prior to reestablishment of connectivity (Tornero et al., 2013). The approach described here fulfills these important criteria, as the formation of graft-derived long-range projections corresponded essentially to the damaged areas, i.e., visual/limbic, and is strikingly similar to results obtained with lesions of the frontal cortex (Gaillard et al., 2007). This high specificity should be of major interest in the context of brain repair, as diffuse or non-specific projections have been proposed to contribute to detrimental secondary effects in better established models of transplantation-mediated brain repair (Gaillard and Jaber, 2011; Lane et al., 2010).

We previously found that grafted cortical neurons derived from ESCs or from embryonic cortex that display mainly an occipital identity prior to grafting establish projections with a predominantly visual and limbic cortical identity, despite the fact that they were grafted in the motor cortex (Gaspard et al., 2008; Gaillard et al., 2003; Pinaudeau et al., 2000). Here, we found that ESC-derived cortical neurons retain their intrinsic areal specification even in the adult brain, which means that optimal restoration of cortical projections requires proper specification of the neurons prior to grafting. On the other hand, in some experimental settings, there appears to be a higher potential for respecification of the transplanted cells by the host neonatal brain, using embryonic cortex (O'Leary et al., 2007) or ESC-derived cortical-like cells (Ideguchi et al., 2010). This could be linked to a different degree of maturation and specification of the transplanted cells, which are expected to lose plasticity with time (Pinaudeau et al., 2000). It will be interesting in the future to determine the mechanisms underlying these differences, which could be used to fine-tune the degree of commitment and plasticity of transplanted cells depending on the type of lesion and desired repair.

Our data also suggest that a precise match is required between the areal identity of the lesioned neurons and that of the grafted neurons to achieve axonal outgrowth to subcortical targets. This is consistent with previous studies using embryonic cortical tissue or cells (Fricker-Gates et al., 2002; Gaillard et al., 2007; Sheen et al., 1999), that have shown that only homotopically grafted motor embryonic cortex, and not heterotopically

grafted visual cortex, can enable the reestablishment of patterns of axonal outgrowth following lesions of the motor cortex.

These observations raise the question of which mechanisms, in the damaged brain, control this specificity, from axon pathfinding to target selection and synaptogenesis. An attractive hypothesis is that, following brain damage and denervation, some specific guidance cues may become re-expressed along defined regional patterns, thereby allowing the newly growing axons to reach their appropriate targets, as previously described following optic nerve lesions (Knöll et al., 2001). The transplant-derived fibers may be also guided by degenerated pathways (Gaillard and Jaber, 2007) or remaining fibers from the damaged area, which could also involve area-specific cues involved in axon-axon recognition and fasciculation. Axonal growth is also likely to be influenced by more permissive spatial constraints of the damaged host. Further understanding of these questions may be of crucial importance to determine the conditions by which neural circuits can be restored physiologically in the lesioned adult brain.

Functional integration of transplanted neurons has been described previously following grafting of embryonic cortical tissue into lesioned adult cortex (Dunnett et al., 1987; Ebrahimi-Gaillard et al., 1995; Santos-Torres et al., 2009), including visual cortex (Gaillard et al., 1998b; Girman, 1994; Girman and Golovina, 1990). Here, we show that a similar functional integration can be achieved using ESC-derived neurons of visual cortex identity, since at least some of these neurons display similar patterns of electrophysiological properties, including, most notably, the capacity to respond to visual stimuli in vivo. It remains to establish which The parts of the visual circuits that are critically involved in these processes have yet to be established. Indeed, our anatomical analyses of axonal and synaptic input and output suggest that at least some of the responses are linked to thalamocortical connectivity, but they may additionally be linked to other sources, such as CL cortex. It will also be interesting to explore in more detail whether the transplanted neurons are only responsive to visual cues or if they may also display broader responsiveness to other sensory cues. Finally, it remains to be tested whether and how such functional responses could contribute to functional restoration at the system level, which remains essentially unknown in most paradigms of brain repair.

In any case, the possibility to reconstruct at least a part of the cortical circuits of visual or limbic identity may be useful for limited clinical applications, such as strokes located in the visual or limbic cortex. It will be most interesting to design protocols of directed differentiation into cortical neurons of specific areal identity that are even more clinically relevant—such as motor cortex, for instance—using in vitro manipulation of known pathways involved in areal specification (Sur and Rubenstein, 2005; Tiberi et al., 2012b; Vanderhaeghen and Polleux, 2004) and test them in similar paradigms of grafting into lesioned adult cortex. Finally, it will be also important to determine whether human ESCs and iPSCs, which can be similarly differentiated into cortical neurons and transplanted into neonatal brain (Espuny-Camacho et al., 2013), can be of potential use for cortical repair, as reported for human iPSC-derived dopaminergic neurons in animal models of Parkinson disease (Hargus et al., 2010; Kriks et al., 2011; Wernig et al., 2008). Thus, our study constitutes an important first step toward the rational design of specific repair of lesions of the adult cerebral cortex, which is a frequent target of neurological diseases.

EXPERIMENTAL PROCEDURES

ES Cell Culture and Differentiation

A tau-GFP ESC line (Tucker et al., 2001) was differentiated into cortical pyramidal neurons as previously described (Gaspard et al., 2009a). After 14 days of differentiation, cells were dissociated prior to grafting, as described for neonatal mouse grafting (Gaspard et al., 2008).

Lesioning and Grafting

All mouse experiments were performed with the approval of the Université Libre de Bruxelles Committee for animal welfare. Six- to 8-week-old adult CD1, C57bl/6, or ubiquitous tdTOMATO mice (Madisen et al., 2010) were anesthetized with ketamine and xylazine, followed by focal stereotactic injections of ibotenic acid to obtain focal lesions. Three days later, 50,000–200,000 ESC-derived cells (in 0.5–1 μl) were injected in the same location. As internal controls, ibotenic-acid-lesioned mice (n = 24) were grafted with embryonic cortical tissue from GFP-expressing embryos as described in Gaillard et al. (2007). For the aspiration lesion group, a part of the left visual cortex was aspirated, followed by grafting of 200,000 cells (in 0.5 μl) into the lesioned cavity.

Immunofluorescence and Immunohistochemistry

For conventional microscopy analysis and quantification, the mice were anesthetized with an overdose of ketamine/xylazine and perfused with PBS followed by 4% paraformaldehyde, followed by post-fixation overnight. The grafts and its projections were visualized with immunofluorescence or immunohistochemical detection of GFP (1:1,000 chicken from Abcam; 1:2,000 rabbit from Invitrogen) or other markers (MAP2 [1:500, mouse, Sigma], FOXP2 [1:500, rabbit, Abcam], Tbr1 [1:500, chicken, Millipore; and 1:5,000, rabbit, a generous gift from R.F. Hevner], SATB2 [1:500, mouse, Abcam], nestin [1:1,000, mouse, Covance], CTIP2 [1:250, rat, Serotec], NeuN [1:500, mouse, Millipore], GFAP [1:500, rabbit, Sigma], COUPTF1 [1:1,000, mouse, Abcam], GAD67 [1:1,000, mouse, Covance], SMI-32 [1:1,000, mouse, Covance], and IBA1 [1:500, rabbit, Wako]) in free-floating sections, as described previously (Gaillard et al., 2007; Gaspard et al., 2008).

Electron Microscopy

For electron microscopy, the anesthesized mice were perfused with a physiological saline solution, followed by 4% paraformaldehyde and 0.2% glutaraldehyde in phosphate buffer, and the brains were cut in 60-μm slices before further processing. For GFP immunogold detection, the sections were incubated in goat antibody to rabbit immunoglobulin G (IgG) conjugated to ultra-small gold particles (0.8 nm, 1:100; Aurion). The immunogold signal was intensified using a silver enhancement kit (HQ Silver, Nanoprobes). Serial ultra-thin immunostained sections were cut with a UC6 ultramicrotome (Leica) and were contrasted with lead citrate and observed in a electron microscope (JEOL).

Axon Tracer Injection

Thalamic input to the graft was traced with the anterograde tracer biotin dextran amine (BDA, 10,000 molecular weight [MW], Molecular Probes). BDA (10% in PBS) was applied iontophoretically (7 μA, 15 min) through glass micropipettes (internal tip diameter, 8–10 μm). Grafted neuron projections were traced using retrograde tracers with dextran conjugated to Alexa Fluor 568 or Alexa Fluor 647 (0.5 ml, 1% in distilled water, Molecular Probes).

Quantification and Statistical Analyses

For cerebral cortex and striatum, the total number of fibers in each specific area was counted in one to five sections per animal. For the thalamus and midbrain, fibers were counted in every second or third section throughout the brain. The localization of the boundaries of the lesion site and surrounding areas was determined following stainings with the pan-neuronal transcription factor NeuN and non-phosphorylated neurofilament protein (SMI-32). To

compare the patterns of output of transplanted neurons with those of host visual cortex following retrograde tracer injections, the areas of interest within the graft and within the adjacent host visual cortex were captured using a 40× objective by laser scanning confocal microscopy (FV1000; Olympus), followed by manual counting of double- and/or triple-labeled neurons. Statistical analyses were performed using the non-parametric Wilcoxon signed-rank test for paired data (when comparing results in different brain areas in the same group of mice) and the Mann-Whitney test for independent data (when comparing results in different groups of mice, i.e., those lesioned and grafted in different locations). A three-way saturated log-linear model was used to compare the proportions of mice with fibers in specific brain regions. The proportion of retrograde tracer positive cells expressing layer-specific markers CTIP2 or FOXP2 were compared with a Student's t test for paired data.

Electrophysiological Recordings and Identification of Recorded Neurons

Three to 9 months following transplantation, extracellular single-unit recordings were obtained from adult control and grafted mice, as described elsewhere (Tseng et al., 2006), with specific modifications described in the Supplemental Experimental Procedures. Light flashes (1,000 lumen, 1 s duration) were performed with a light bulb placed 40 cm from the eye CL to the recorded visual cortex. Electrophysiological recordings were analyzed offline using Spike2 software sorting detection protocol to discriminate individual neurons based on waveform template matching. Intrinsic properties of recorded neurons (AP duration, firing frequency) were analyzed over a 1-min baseline recording just before stimulations. A peristimulus time histogram was used to analyze the firing frequency before and after light stimulation. Mean firing frequencies were measured 700 ms before and after light stimulation using Spike2 software.

Following each recording, neurons were iontophoretically labeled with neurobiotin as described elsewhere (Henny et al., 2012; Pinault, 1996), followed by brain fixation and vibrosection, and GFP/biotin double immunolabeling. For subsequent analyses displayed in Table S1, only recorded neurons showing unambiguous GFP expression were included.

Gene Expression Analysis

E16 frontal and occipital cortices were dissected from four independent litters, used as four replicates. RNA extraction, DNase treatment, retrotranscription, and qPCR were performed as in van den Ameele et al., (2012), using primers described in Supplemental Experimental Procedures.

SUPPLEMENTAL INFORMATION

Supplemental Information includes eight figures, one table, and Supplemental Experimental Procedures and can be found with this article online at http://dx.doi.org/10.1016/j.neuron.2015.02.001.

AUTHOR CONTRIBUTIONS

K.A.M. and S.A.-V. performed all experiments, with the help of A.G., M.B.-M., I.E.-C., N.G., and B.S. A.G. and P.V. designed and analyzed all experiments and wrote the manuscript, with the help of K.A.M., S.A.-V., and M.B.-M.

ACKNOWLEDGMENTS

We thank Gilbert Vassart for continuous support and interest; members of the lab and IRIBHM for helpful discussions and advice; Viviane De Maertelaer for advice on statistical analyses; E. Béré for advice on electron microscopy and ImageUP for microscopy; and Jean-Marie Vanderwinden of the Light Microscopy Facility (LiMiF) for support with imaging. This work was funded by grants from the Belgian Fonds National de la Recherche Scientifique (FNRS) and Fonds de la Recherche en Sciences Medicales (FRSM); the Belgian Queen Elizabeth Medical Foundation; the Interuniversity Attraction Poles Program (IUAP); WELBIO and Programme d'Excellence CIBLES of the Walloon Region; the Fondations Clerdent and de Spoelbergh; the AXA Research Fund; Fondation ULB (to P.V.); Fondation de France; and the Agence Nationale de la Recherche (ANR) (grant ANR-09-MNPS-027-01 and FEDER number 33552 to A.G.). I.E.-C. was a post-doctoral fellow of the FNRS. B.S. is a post-doctoral fellow of the ANR.

Received: November 21, 2013
Revised: December 18, 2014
Accepted: January 27, 2015
Published: March 4, 2015

REFERENCES

Aboody, K., Capela, A., Niazi, N., Stern, J.H., and Temple, S. (2011). Translating stem cell studies to the clinic for CNS repair: current state of the art and the need for a Rosetta stone. Neuron *70*, 597–613.

Anderson, S., and Vanderhaeghen, P. (2014). Cortical neurogenesis from pluripotent stem cells: complexity emerging from simplicity. Curr. Opin. Neurobiol. *27*, 151–157.

Arlotta, P., and Berninger, B. (2014). Brains in metamorphosis: reprogramming cell identity within the central nervous system. Curr. Opin. Neurobiol. *27*, 208–214.

Cang, J., Kaneko, M., Yamada, J., Woods, G., Stryker, M.P., and Feldheim, D.A. (2005). Ephrin-as guide the formation of functional maps in the visual cortex. Neuron *48*, 577–589.

Chiba, S., Ikeda, R., Kurokawa, M.S., Yoshikawa, H., Takeno, M., Nagafuchi, H., Tadokoro, M., Sekino, H., Hashimoto, T., and Suzuki, N. (2004). Anatomical and functional recovery by embryonic stem cell-derived neural tissue of a mouse model of brain damage. J. Neurol. Sci. *219*, 107–117.

Cusulin, C., Monni, E., Ahlenius, H., Wood, J., Brune, J.C., Lindvall, O., and Kokaia, Z. (2012). Embryonic stem cell-derived neural stem cells fuse with microglia and mature neurons. Stem Cells *30*, 2657–2671.

Dunnett, S.B., Ryan, C.N., Levin, P.D., Reynolds, M., and Bunch, S.T. (1987). Functional consequences of embryonic neocortex transplanted to rats with prefrontal cortex lesions. Behav. Neurosci. *101*, 489–503.

Ebrahimi-Gaillard, A., Beck, T., Gaillard, F., Wree, A., and Roger, M. (1995). Transplants of embryonic cortical tissue placed in the previously damaged frontal cortex of adult rats: local cerebral glucose utilization following execution of forelimb movements. Neuroscience *64*, 49–60.

Eiraku, M., Watanabe, K., Matsuo-Takasaki, M., Kawada, M., Yonemura, S., Matsumura, M., Wataya, T., Nishiyama, A., Muguruma, K., and Sasai, Y. (2008). Self-organized formation of polarized cortical tissues from ESCs and its active manipulation by extrinsic signals. Cell Stem Cell *3*, 519–532.

Espuny-Camacho, I., Michelsen, K.A., Gall, D., Linaro, D., Hasche, A., Bonnefont, J., Bali, C., Orduz, D., Bilheu, A., Herpoel, A., et al. (2013). Pyramidal neurons derived from human pluripotent stem cells integrate efficiently into mouse brain circuits in vivo. Neuron *77*, 440–456.

Fricker-Gates, R.A., Shin, J.J., Tai, C.C., Catapano, L.A., and Macklis, J.D. (2002). Late-stage immature neocortical neurons reconstruct interhemispheric connections and form synaptic contacts with increased efficiency in adult mouse cortex undergoing targeted neurodegeneration. J. Neurosci. *22*, 4045–4056.

Friling, S., Andersson, E., Thompson, L.H., Jönsson, M.E., Hebsgaard, J.B., Nanou, E., Alekseenko, Z., Marklund, U., Kjellander, S., Volakakis, N., et al. (2009). Efficient production of mesencephalic dopamine neurons by Lmx1a expression in embryonic stem cells. Proc. Natl. Acad. Sci. USA *106*, 7613–7618.

Gaillard, A., and Jaber, M. (2007). Is the outgrowth of transplant-derived axons guided by host astrocytes and myelin loss? Cell Adhes. Migr. *1*, 161–164.

Gaillard, A., and Jaber, M. (2011). Rewiring the brain with cell transplantation in Parkinson's disease. Trends Neurosci. *34*, 124–133.

Gaillard, A., Gaillard, F., and Roger, M. (1998a). Neocortical grafting to newborn and adult rats: developmental, anatomical and functional aspects. Adv. Anat. Embryol. Cell Biol. *148*, 1–86.

Gaillard, F., Girman, S.V., and Gaillard, A. (1998b). Afferents to visually responsive grafts of embryonic occipital neocortex tissue implanted into V1 (Oc1) cortical area of adult rats. Restor. Neurol. Neurosci. *12*, 13–25.

Gaillard, A., Nasarre, C., and Roger, M. (2003). Early (E12) cortical progenitors can change their fate upon heterotopic transplantation. Eur. J. Neurosci. *17*, 1375–1383.

Gaillard, F., Domballe, L., and Gaillard, A. (2004). Fetal cortical allografts project massively through the adult cortex. Neuroscience *126*, 631–637.

Gaillard, A., Prestoz, L., Dumartin, B., Cantereau, A., Morel, F., Roger, M., and Jaber, M. (2007). Reestablishment of damaged adult motor pathways by grafted embryonic cortical neurons. Nat. Neurosci. *10*, 1294–1299.

Gaspard, N., Bouschet, T., Hourez, R., Dimidschstein, J., Naeije, G., van den Ameele, J., Espuny-Camacho, I., Herpoel, A., Passante, L., Schiffmann, S.N., et al. (2008). An intrinsic mechanism of corticogenesis from embryonic stem cells. Nature *455*, 351–357.

Gaspard, N., Bouschet, T., Herpoel, A., Naeije, G., van den Ameele, J., and Vanderhaeghen, P. (2009a). Generation of cortical neurons from mouse embryonic stem cells. Nat. Protoc. *4*, 1454–1463.

Gaspard, N., Gaillard, A., and Vanderhaeghen, P. (2009b). Making cortex in a dish: in vitro corticopoiesis from embryonic stem cells. Cell Cycle *8*, 2491–2496.

Gates, M.A., Fricker-Gates, R.A., and Macklis, J.D. (2000). Reconstruction of cortical circuitry. Prog. Brain Res. *127*, 115–156.

Girman, S.V. (1994). Neocortical grafts receive functional afferents from the same neurons of the thalamus which have innervated the visual cortex replaced by the graft in adult rats. Neuroscience *60*, 989–997.

Girman, S.V., and Golovina, I.L. (1990). Electrophysiological properties of embryonic neocortex transplants replacing the primary visual cortex of adult rats. Brain Res. *523*, 78–86.

Guitet, J., Garnier, C., Ebrahimi-Gaillard, A., and Roger, M. (1994). Efferents of frontal or occipital cortex grafted into adult rat's motor cortex. Neurosci. Lett. *180*, 265–268.

Hargus, G., Cooper, O., Deleidi, M., Levy, A., Lee, K., Marlow, E., Yow, A., Soldner, F., Hockemeyer, D., Hallett, P.J., et al. (2010). Differentiated Parkinson patient-derived induced pluripotent stem cells grow in the adult rodent brain and reduce motor asymmetry in Parkinsonian rats. Proc. Natl. Acad. Sci. USA *107*, 15921–15926.

Henny, P., Brown, M.T., Northrop, A., Faunes, M., Ungless, M.A., Magill, P.J., and Bolam, J.P. (2012). Structural correlates of heterogeneous in vivo activity of midbrain dopaminergic neurons. Nat. Neurosci. *15*, 613–619.

Hernit-Grant, C.S., and Macklis, J.D. (1996). Embryonic neurons transplanted to regions of targeted photolytic cell death in adult mouse somatosensory cortex re-form specific callosal projections. Exp. Neurol. *139*, 131–142.

Ideguchi, M., Palmer, T.D., Recht, L.D., and Weimann, J.M. (2010). Murine embryonic stem cell-derived pyramidal neurons integrate into the cerebral cortex and appropriately project axons to subcortical targets. J. Neurosci. *30*, 894–904.

Isacson, O., Wictorin, K., Fischer, W., Sofroniew, M.V., and Björklund, A. (1988). Fetal cortical cell suspension grafts to the excitotoxically lesioned neocortex: anatomical and neurochemical studies of trophic interactions. Prog. Brain Res. *78*, 13–26.

Kim, J.H., Auerbach, J.M., Rodríguez-Gómez, J.A., Velasco, I., Gavin, D., Lumelsky, N., Lee, S.H., Nguyen, J., Sánchez-Pernaute, R., Bankiewicz, K., and McKay, R. (2002). Dopamine neurons derived from embryonic stem cells function in an animal model of Parkinson's disease. Nature *418*, 50–56.

Knöll, B., Isenmann, S., Kilic, E., Walkenhorst, J., Engel, S., Wehinger, J., Bähr, M., and Drescher, U. (2001). Graded expression patterns of ephrin-As in the superior colliculus after lesion of the adult mouse optic nerve. Mech. Dev. *106*, 119–127.

Kriks, S., Shim, J.W., Piao, J., Ganat, Y.M., Wakeman, D.R., Xie, Z., Carrillo-Reid, L., Auyeung, G., Antonacci, C., Buch, A., et al. (2011). Dopamine neurons derived from human ES cells efficiently engraft in animal models of Parkinson's disease. Nature *480*, 547–551.

Lamba, D.A., Gust, J., and Reh, T.A. (2009). Transplantation of human embryonic stem cell-derived photoreceptors restores some visual function in Crx-deficient mice. Cell Stem Cell *4*, 73–79.

Lane, E.L., Björklund, A., Dunnett, S.B., and Winkler, C. (2010). Neural grafting in Parkinson's disease unraveling the mechanisms underlying graft-induced dyskinesia. Prog. Brain Res. *184*, 295–309.

Ma, L., Hu, B., Liu, Y., Vermilyea, S.C., Liu, H., Gao, L., Sun, Y., Zhang, X., and Zhang, S.C. (2012). Human embryonic stem cell-derived GABA neurons correct locomotion deficits in quinolinic acid-lesioned mice. Cell Stem Cell *10*, 455–464.

Madisen, L., Zwingman, T.A., Sunkin, S.M., Oh, S.W., Zariwala, H.A., Gu, H., Ng, L.L., Palmiter, R.D., Hawrylycz, M.J., Jones, A.R., et al. (2010). A robust and high-throughput Cre reporting and characterization system for the whole mouse brain. Nat. Neurosci. *13*, 133–140.

Niell, C.M., and Stryker, M.P. (2008). Highly selective receptive fields in mouse visual cortex. J. Neurosci. *28*, 7520–7536.

O'Leary, D.D., and Sahara, S. (2008). Genetic regulation of arealization of the neocortex. Curr. Opin. Neurobiol. *18*, 90–100.

O'Leary, D.D., Chou, S.J., and Sahara, S. (2007). Area patterning of the mammalian cortex. Neuron *56*, 252–269.

Pinaudeau, C., Gaillard, A., and Roger, M. (2000). Stage of specification of the spinal cord and tectal projections from cortical grafts. Eur. J. Neurosci. *12*, 2486–2496.

Pinault, D. (1996). A novel single-cell staining procedure performed in vivo under electrophysiological control: morpho-functional features of juxtacellularly labeled thalamic cells and other central neurons with biocytin or Neurobiotin. J. Neurosci. Methods *65*, 113–136.

Roy, N.S., Cleren, C., Singh, S.K., Yang, L., Beal, M.F., and Goldman, S.A. (2006). Functional engraftment of human ES cell-derived dopaminergic neurons enriched by coculture with telomerase-immortalized midbrain astrocytes. Nat. Med. *12*, 1259–1268.

Santos-Torres, J., Heredia, M., Riolobos, A.S., Jiménez-Díaz, L., Gómez-Bautista, V., de la Fuente, A., Criado, J.M., Navarro-López, J., and Yajeya, J. (2009). Electrophysiological and synaptic characterization of transplanted neurons in adult rat motor cortex. J. Neurotrauma *26*, 1593–1607.

Schwarcz, R., Hökfelt, T., Fuxe, K., Jonsson, G., Goldstein, M., and Terenius, L. (1979). Ibotenic acid-induced neuronal degeneration: a morphological and neurochemical study. Exp. Brain Res. *37*, 199–216.

Sheen, V.L., Arnold, M.W., Wang, Y., and Macklis, J.D. (1999). Neural precursor differentiation following transplantation into neocortex is dependent on intrinsic developmental state and receptor competence. Exp. Neurol. *158*, 47–62.

Shi, Y., Kirwan, P., Smith, J., Robinson, H.P., and Livesey, F.J. (2012). Human cerebral cortex development from pluripotent stem cells to functional excitatory synapses. Nat. Neurosci. *15*, 477–486.

Sørensen, J.C., Dalmau, I., Zimmer, J., and Finsen, B. (1996a). Microglial reactions to retrograde degeneration of tracer-identified thalamic neurons after frontal sensorimotor cortex lesions in adult rats. Exp. Brain Res. *112*, 203–212.

Sørensen, J.C., Grabowski, M., Zimmer, J., and Johansson, B.B. (1996b). Fetal neocortical tissue blocks implanted in brain infarcts of adult rats interconnect with the host brain. Exp. Neurol. *138*, 227–235.

Sur, M., and Rubenstein, J.L. (2005). Patterning and plasticity of the cerebral cortex. Science *310*, 805–810.

Tabar, V., Panagiotakos, G., Greenberg, E.D., Chan, B.K., Sadelain, M., Gutin, P.H., and Studer, L. (2005). Migration and differentiation of neural precursors derived from human embryonic stem cells in the rat brain. Nat. Biotechnol. *23*, 601–606.

Tiberi, L., van den Ameele, J., Dimidschstein, J., Piccirilli, J., Gall, D., Herpoel, A., Bilheu, A., Bonnefont, J., Iacovino, M., Kyba, M., et al. (2012a). BCL6 controls neurogenesis through Sirt1-dependent epigenetic repression of selective Notch targets. Nat. Neurosci. *15*, 1627–1635.

Tiberi, L., Vanderhaeghen, P., and van den Ameele, J. (2012b). Cortical neurogenesis and morphogens: diversity of cues, sources and functions. Curr. Opin. Cell Biol. *24*, 269–276.

Tornero, D., Wattananit, S., Grønning Madsen, M., Koch, P., Wood, J., Tatarishvili, J., Mine, Y., Ge, R., Monni, E., Devaraju, K., et al. (2013). Human induced pluripotent stem cell-derived cortical neurons integrate in stroke-injured cortex and improve functional recovery. Brain *136*, 3561–3577.

Tseng, K.Y., Mallet, N., Toreson, K.L., Le Moine, C., Gonon, F., and O'Donnell, P. (2006). Excitatory response of prefrontal cortical fast-spiking interneurons to ventral tegmental area stimulation in vivo. Synapse *59*, 412–417.

Tucker, K.L., Meyer, M., and Barde, Y.A. (2001). Neurotrophins are required for nerve growth during development. Nat. Neurosci. *4*, 29–37.

van den Ameele, J., Tiberi, L., Bondue, A., Paulissen, C., Herpoel, A., Iacovino, M., Kyba, M., Blanpain, C., and Vanderhaeghen, P. (2012). Eomesodermin induces Mesp1 expression and cardiac differentiation from embryonic stem cells in the absence of Activin. EMBO Rep. *13*, 355–362.

van den Ameele, J., Tiberi, L., Vanderhaeghen, P., and Espuny-Camacho, I. (2014). Thinking out of the dish: what to learn about cortical development using pluripotent stem cells. Trends Neurosci. *37*, 334–342.

Vanderhaeghen, P. (2012). Generation of cortical neurons from pluripotent stem cells. Prog. Brain Res. *201*, 183–195.

Vanderhaeghen, P., and Polleux, F. (2004). Developmental mechanisms patterning thalamocortical projections: intrinsic, extrinsic and in between. Trends Neurosci. *27*, 384–391.

Wernig, M., Zhao, J.P., Pruszak, J., Hedlund, E., Fu, D., Soldner, F., Broccoli, V., Constantine-Paton, M., Isacson, O., and Jaenisch, R. (2008). Neurons derived from reprogrammed fibroblasts functionally integrate into the fetal brain and improve symptoms of rats with Parkinson's disease. Proc. Natl. Acad. Sci. USA *105*, 5856–5861.

Yang, D., Zhang, Z.J., Oldenburg, M., Ayala, M., and Zhang, S.C. (2008). Human embryonic stem cell-derived dopaminergic neurons reverse functional deficit in parkinsonian rats. Stem Cells *26*, 55–63.

Ying, Q.L., Nichols, J., Evans, E.P., and Smith, A.G. (2002). Changing potency by spontaneous fusion. Nature *416*, 545–548.